NASA TECHNICAL MEMORANDUM

NASA TM X-1403

NASA TM X-1403

SEARCH FOR THE γ-2γ PROCESS IN NUCLEAR ELECTROSTATIC FIELDS

by William K. Roberts and David C. Liu

Lewis Research Center
Cleveland, Ohio

NATIONAL AERONAUTICS AND SPACE ADMINISTRATION • WASHINGTON, D. C. • AUGUST 1967

NASA TM X-1403

SEARCH FOR THE γ-2γ PROCESS IN NUCLEAR ELECTROSTATIC FIELDS

By William K. Roberts and David C. Liu

Lewis Research Center
Cleveland, Ohio

NATIONAL AERONAUTICS AND SPACE ADMINISTRATION

For sale by the Clearinghouse for Federal Scientific and Technical Information
Springfield, Virginia 22151 – CFSTI price $3.00

SEARCH FOR THE γ-2γ PROCESS IN NUCLEAR ELECTROSTATIC FIELDS

by William K. Roberts and David C. Liu

Lewis Research Center

SUMMARY

An experiment designed to detect the γ-2γ process (an interaction of a photon with an electric field with the subsequent emission of two photons) was performed. A geometry was chosen in which the secondary gamma rays were emitted at an angle of 90° to each other and at an angle of 135° to the projection of the incident gamma ray arrival direction. Measurements were performed by using lead and copper targets and 1.33-MeV (2.14×10^{-13} J) primary gamma rays. An energy-summing time-coincidence technique was employed to detect pairs of secondary gamma rays. Statistically significant upper limits of 960 nanobarns per steradian squared per MeV (6×10^{-22} $m^2/(sr^2)(J)$) for the differential cross section in lead and 146 nanobarns per steradians squared per MeV (0.915×10^{-22} $m^2/(sr^2)(J)$) in copper were obtained, comparing with theoretical values of 0.8 and 0.1 nanobarn per steradian squared per MeV (0.5×10^{-24} and 0.062×10^{-24} $m^2/(sr^2)(J)$), respectively, for this geometry. Although the upper limits established herein did not become a rigorous test of the theory, information gained from this experiment indicate that cross sections in the range of theoretical predictions can be measured with suitable improvements of the experimental technique. These improvements are discussed herein.

INTRODUCTION

Quantum electrodynamics predicts a number of effects involving the interaction of electromagnetic radiation (photons) with an electric field. One such effect is a change in the state of the vacuum, commonly referred to as "vacuum polarization." While not directly observable, polarization of the vacuum will affect a number of observable processes by calculable amounts. Data for one such process, a shift in the atomic level of an electron (ref. 1) the Lamb shift), are in excellent agreement with calculated values (ref. 2). However, it is also of interest to observe other processes affected by vacuum polarization such as photon-photon scattering (refs. 3 and 4), Delbruck scattering (ref. 5), and a process in which a photon interacts with an electrostatic field (usually the

nuclear electrostatic field) with the subsequent emission of two photons (γ-2γ process (refs. 6 to 9).

The calculated cross section for the first process is small and difficult to verify because sufficiently intense photon sources are not available except perhaps in laser beams. Delbruck scattering, on the other hand, has an appreciable cross section but because of the lack of a sufficiently detailed theoretical knowledge of scattering amplitudes and relative phases, it cannot be distinguished from other coherent processes (Thomson and Rayleigh scatterings). At very high energies, however, where Delbruck scattering is the dominant process, experimental results seem to confirm theoretical predictions but not without some statistical uncertainty (refs. 10 and 11).

The cross section for the γ-2γ process is small. However, the coincidence requirement which can be placed on the secondary gamma rays, coupled with the condition that in a nuclear encounter the secondary gamma rays retain essentially the total primary gamma-ray energy, makes this process experimentally attractive. Two double Compton scattering processes, one from atomic electrons and the other from the nuclei, could compete with the γ-2γ process. However, neither process competes seriously, the first because, in the geometry used herein, the energy available to the secondary gamma rays is too small and the second because the estimated cross section (ref. 11) is about three orders of magnitude smaller than the γ-2γ cross section.

This report describes an experimental search for the γ-2γ process employing a gamma-ray energy-summing time-coincidence experimental technique.

CHOICE OF GEOMETRY AND PRIMARY GAMMA RAY ENERGY

Figure 1 shows the geometry employed in this experiment. A source of gamma rays of energy E_0 is enclosed in a lead shield. A collimator integrally attached to the shield allows a beam of gamma rays to emerge and impinge on the target which provides the nuclear electrostatic field for the interaction. The secondary gamma rays associated with the γ-2γ process are detected by two gamma-ray detectors situated at mean angles θ_1 and θ_2 with respect to the center of the target and the projection of the primary photon arrival direction (symbols are defined in appendix A). The mean angle between the detectors, with the vertex at the target, is denoted by θ_{12}. Hereinafter, the geometry is denoted by reference to the angles $(\theta_1, \theta_2, \theta_{12})$.

Calculations of the γ-2γ cross section have been made by Bolsterli (ref. 7), Talman (ref. 8), and Shima (ref. 9). Shima's work is a more exact calculation than those presented by either Bolsterli or Talman. Unfortunately, it became available only after the bulk of experimental data was obtained. Any future experiments should be performed in geometries favored by Shima's calculations. All three calculations show that

the cross section $d^2\sigma_{2\gamma}/d\Omega_1\, d\Omega_2$ is proportional to the target nuclear charge squared Z^2 and to E_0^6 provided $E_0 \ll m_0c^2 = 0.51$ MeV (0.82×10^{-13} J). At higher energies such as those employed in this experiment, the exact energy dependence is different and is properly accounted for only in the calculations of Shima. At these energies, the calculated cross sections in references 7 to 9 are in general agreement for a geometry of (90^o, 90^o, 180^o). For other geometries, the calculation of Shima predicts much smaller cross sections than those of Bolsterli or Talman.

Figure 2(a) is a plot of the differential cross section $d^3\sigma_{2\gamma}/d\Omega_1\, d\Omega_2\, dE_1$ against secondary photon energy E_1 as calculated by Bolsterli and by Shima for a (90^o, 90^o, 180^o) geometry. Figure 2(b) is a similar plot for a (135^o, 135^o, 90^o) geometry. For both geometries, $E_0 = 1.33$ MeV (2.14×10^{-13} J). For asymmetric geometries ($\theta_1 \neq \theta_2$), the differential cross section is asymmetric; that is, the average energy of the gamma rays radiated at the larger angle is less than $E_0/2$ and the average energy of the gamma rays radiated at the smaller angle is more than $E_0/2$.

In addition to gamma rays associated with the γ-2γ process, the detectors shown in figure 1 detect many other gamma rays whose energies are dependent on θ_1, θ_2, and E_0. There are also contributions to the photon flux from the bremsstrahlung process in the target, room background radiation, and other higher order processes. Cosmic rays can also deposit energy in the detectors but contribute relatively few gamma rays to the flux of photons seen by each detector.

Figure 3 shows a schematic plot of the photon flux $\varphi(E)$ in the vicinity of a detector located at a mean angle θ_1. The peak at

$$E_c = \frac{E_0}{1 + \dfrac{E_0}{m_0c^2}(1 - \cos\theta_1)}$$

is a result of Compton scattering of primary gamma rays in the target toward the detector. The peak is broad because neither the detector nor the target is a point so that the Compton scattered gamma ray may scatter through angles both larger and smaller than θ_1. If $E_0 > 2m_0c^2 = 1.02$ MeV (1.64×10^{-13} J) production of positron-electron pairs can occur in the target, and the subsequent annihilation of the positron produces two gamma rays of energy $E_A = 0.51$ MeV (0.82×10^{-13} J). Thus, pair production adds a monoenergetic gamma ray component of energy E_A to the total gamma ray flux. The continuum portion of the flux is a result of bremsstrahlung processes in the target, room background radiation, and other high order processes. The energy tail in the region greater than E_0 has its origin in room background radiation.

The experimental procedure used in measuring the cross section consisted of detecting pairs of gamma rays coherently produced in the target which deposited a fixed sum energy equal to E_0 coincidently in the two detectors. Chance coincidence can occur in a detection system operated in this manner at a rate $R_{ch} = 2\tau R_1 R_2$, where R_1 and R_2 are the average rates at which gamma rays interact in the two detectors and τ is the resolution time of the coincidence circuit. It is possible, however, to select experimentally only gamma rays in fixed energy intervals. Therefore, the chance-coincidence events selected and, consequently, the chance-coincidence rate can be altered electronically. Estimates showed that approximately 10^8 Compton scattered gamma rays would impinge on a detector for every gamma ray associated with a γ-2γ event. For this reason, it was necessary to exclude electronically Compton scattered gamma rays to obtain as large a true- to change-coincidence-rate ratio as possible.

If $E_0 > 1.02$ MeV (1.64×10^{-13} J), annihilation radiation is produced. Annihilation radiation can affect the experiment adversely for two reasons which bear on the selection of E_0 and the energy of the secondary gamma rays.

If E_0 is much larger than 1.02 MeV (1.64×10^{-13} J), the intensity of annihilation gamma-ray radiation incident on a detector becomes appreciable and must be excluded electronically from detection to preserve as large a true- to chance-coincidence ratio as possible. In lead, the intensity of annihilation radiation is about 10 percent of the Compton scattered gamma-ray intensity for $E_0 = 1.5$ MeV (2.40×10^{-13} J). For an E_0 less than this, the contribution to the chance-coincidence rate caused by annihilation radiation is negligible.

If annihilation radiation is produced in the target, "chance-true" coincident events would be produced which cannot be removed by chance-coincidence subtraction. Such events arise from the combination of the following events:

(1) Detection of the total energy of one annihilation gamma ray in detector 1 and the other annihilation gamma ray after it has Compton scattered in the target into detector 2

(2) Precedent or subsequent pileup in detector 2 of a Compton scattered primary gamma ray within the time resolution of the coincidence circuitry

The annihilation event alone would cause a true coincidence but would not be observed because it does not meet the energy requirement of the energy discrimination windows. The addition of the pileup event in detector 2, however, would satisfy the energy requirement of discriminator 2. Consequently, the combination of events (1) and (2) gives chance-true coincidence events which cannot be distinguished from a true coincidence event without changing source strength or geometry. Further examination of the problem indicated that there is no experimentally usable geometry for which events of this kind have a sum energy much different from 1.15 MeV (1.84×10^{-13} J), independent of E_0 for $E_0 > 1.02$ MeV (1.64×10^{-13} J). Consequently, E_0 must not be chosen near 1.15 MeV

(0.74×10^{-13} J) to prevent the identification of the chance-true events as true γ-2γ events. A source with a gamma-ray energy either below 1.02 MeV (1.64×10^{-13} J) or somewhat greater than 1.15 MeV (1.84×10^{-13} J) must be used.

A lower limit may be placed on acceptable values of E_0. Since the energy discrimination window must not accept pulses of energy less than or equal to E_c, only those E_0 for which $E_0 - \Delta E$ is greater than $2E_c$ are satisfactory. When reasonable values of E_c = 0.30 MeV (0.48×10^{-13} J) and ΔE = 0.20 MeV (0.32×10^{-13} J) are assumed, the lower limit is $E_0 \geq 0.80$ MeV (1.28×10^{-13} J). The source of primary gamma rays chosen for this experiment was cobalt 60, which emits a pair of gamma rays in cascade of energies E_0 = 1.17 (1.87×10^{-13} J) and 1.33 MeV (2.14×10^{-13} J). The gamma ray of interest in the experiment was the 1.33-MeV (2.14×10^{-13} J) energy because of the monotonically increasing dependence of cross section on energy. This energy was high enough that chance-true events could not be mistaken for true γ-2γ events but not high enough to produce any appreciable increase in the chance-coincidence rate. A gamma-ray source in the energy range $0.80 < E_0 < 1.02$ MeV ($1.28\times10^{-13} < \epsilon_0 < 1.64\times10^{-18}$ J) was not chosen on the basis of the energy dependence of cross section.

In the design of this experiment, there were still other factors related to the choice of geometry and/or energy. The gamma-ray detectors must not be placed on a centerline through the target, or coincident-annihilation gamma rays would be detected. Moreover, the detectors must be shielded from each other to eliminate single gamma-ray scatterings between detectors which would also produce unwanted time-coincidence events. Geometries in which $\theta_1 \neq \theta_2$ are unfavorable because, as previously mentioned, the average energy of the secondary gamma rays associated with the larger angle is less than $E_0/2$. This inequality would reduce the probability that a gamma ray of a pair detected by that detector would have an energy greater than E_c and, consequently, reduces the true- to chance-coincidence-rate ratio.

The actual geometry employed in this experiment is shown in figure 4. This geometry (135°, 135°, 90°) minimizes detector to target distance, provides adequate shielding between detectors, and minimizes the maximum Compton scattered gamma-ray energy to $E_c < 0.26$ MeV (0.16×10^{-13} J). Two targets, 0.319 centimeter wide, 7.62 centimeter high, and 2.54 centimeter deep, were employed and staggered as shown in figure 4. Staggering the targets in this manner preserved the total frontal area of the target and reduced absorption of secondary gamma rays in the target.

Figure 2(b) shows that $d^3\sigma_{2\gamma}/d\Omega_1\, d\Omega_2\, dE_1$ has a broad maximum in the region of $E_1 = E_0/2$. Consequently, if the gamma rays which deposited energy between $(E_0 - \Delta E)/2$ and $(E_0 + \Delta E)/2$ are selected from among those incident on detectors 1 and 2, and ΔE is chosen so that it encompasses a major portion of $d^3\sigma_{2\gamma}/d\Omega_1\, d\Omega_2\, dE_1$, while excluding Compton scattered gamma-ray energies, a maximum true- to chance-coincidence-rate ratio would be obtained. This is because the major contribution to the chance-coincidence

rate arises from Compton gamma rays. Electronically, ΔE is referred to as the "energy discrimination window," and is set equal to 0.44 MeV (0.71×10^{-13} J) in this experiment. If Shima's calculations had been available previous to this experiment, a more favorable geometry based on his calculations would have been chosen.

ELECTRONICS

A block diagram of the electronics employed is shown in figure 5. The energy signals from the 5.08 centimeter diameter by 5.08 centimeter high sodium iodide (T1)-photomultiplier-tube gamma-ray detectors were amplified by double delay-line clipped amplifiers. The outputs from the amplifiers were sent to a pulse-height summing amplifier and to individual, fast, single-channel pulse-height selectors. The pulse-height selector outputs fed a coincidence circuit which, in turn, operated a linear gate in the sum channel. The energy sum pulses allowed through the linear gate were sorted according to pulse height and stored in a multichannel pulse-height analyzer memory. Estimates of $d^3\sigma_{2\gamma}/d\Omega_1\, d\Omega_2\, dE_1$ were made from an analysis of the energy spectrum of the coincident events stored in the memory.

The gains of detector-amplifier chains 1 and 2 were equalized by adjusting the gain of either amplifier 1 or 2. The coincidence circuit employed had a resolution time 2τ of 45 nanoseconds. Time-coincident events were detected with 100 percent efficiency with a resolution time of 40 nanoseconds, but a time of 45 nanoseconds was chosen in the actual experiment to eliminate any long term drift or temperature effects. Periodic detector-amplifier gain checks were made throughout the duration of a measurement, and the overall gain varied less than 2 percent in any given run. Pulse-height selector stability was at least as good.

Pulses from either detector could be gated into the analyzer by the corresponding single-channel pulse-height selector. The singles spectra were needed to generate the chance-coincidence contribution to the experimental pulse-height distribution.

To determine whether any background coincidence events occurred in the absence of source and/or target, data were accumulated over varying lengths of time (1) with source but without target, (2) with target but without source, and (3) with neither source nor target in position. In each case, a similar background energy-summing-time-coincidence spectrum was observed which is attributed to cosmic-ray coincidences in the two detectors. No direct proof of the cosmic-ray origin of this background was obtained. However, the facts that additional absorber placed between the detectors did not decrease the observed background and that delaying one pulse-height selector signal enough to eliminate all true-coincidence events removed this background were used to infer its cosmic-ray origin.

RESULTS

As shown with more detail in appendix B, the average differential γ-2γ cross section per atom over the energy discrimination window ΔE can be computed from the equation

$$\frac{\overline{d^3\sigma_{2\gamma}}}{d\Omega_1\, d\Omega_2\, dE} = \frac{\sigma_T N(E_0)}{N_\gamma\, \Delta E p(\Delta E, E_0)} \tag{A6}$$

where σ_T is the total gamma-ray interaction cross section for target nuclei in nanobarns per atom (m^2/atom), $N(E_0)$ is the number of detected coincidence events which deposit in the two detectors a sum energy equal to E_0, N_γ is the total number of primary gamma rays that interact in the target during the period of observation, ΔE is the energy discrimination windows in units of MeV, and $p(\Delta E, E_0)$ is the average detection efficiency in units of steradians squared for detecting the total energy carried by a γ-2γ pair with energies lying in ΔE.

Figure 6 shows the experimental energy-summing time-coincidence spectra obtained for copper and lead targets. These data were obtained by using radioactive cobalt 60 as the source of primary gamma rays ($E_0 = 1.33$ MeV, 2.14×10^{-13} J). The source strength was 0.25 curie or $\sim0.9\times10^{10}$ decays per second. The data were accumulated over an interval of 5120 minutes.

A chance-coincidence pulse-height spectrum for each target was generated by using energy discriminator-gated, individual pulse-height spectra as outlined in appendix C. The sum of the computed chance-coincidence spectrum and a least-squares-fitted cosmic-ray-background spectrum is also plotted in figure 6. The difference between the observed and the composite background is the true energy-summing time-coincidence spectrum.

It is obvious from the data shown in figure 6 that, if a peak exists at 1.33 MeV (2.14×10^{-13} J), it must be very small. Consequently, an attempt was made to set a lower limit on the number of coincidence events $N(E_0)$ which could have been observed. The following chi-square test was performed for this purpose. The shape of a sum peak was experimentally determined by using 1.33-MeV (2.14×10^{-13} J) gamma rays Compton scattered from one detector into the other. A set of sum peaks was generated from this curve and was added to the background curves of figure 6. The resulting curve is referred to as a "test curve." Values of chi-square test were then obtained from the raw data and each of the test curves. The test hypothesis for each chi-square value is that the experimental data are a random sample from a population given by the test curves.

The insets in figure 6 show the sum peaks for which the chi-square test resulted in a rejection of this hypothesis at a significance level of 0.05. This rejection amounts to the assertion that, if there were an actual peak of this shape, there is at most a 5 percent chance that the data constitute a sample from the population shown in the test curve.

The area $N(E_0)$ under a sum-peak curve is the quantity which actually enters the cross-section computations; therefore, the results of this chi-square test permit the setting of an upper limit on the true γ-2γ cross section by using in equation (A6) the $N(E_0)$ from the test curve. The best values of $N(E_0)$ obtained from these measurements are summarized in table I along with values of N_γ, σ_T, ΔE, $p(\Delta E, E_0)$. The statistical upper limits of $\overline{d^3\sigma_{2\gamma}/d\Omega_1\, d\Omega_2\, dE_1}$ for copper and lead are 146 and 960 nanobarns per steradians squared per MeV (0.91×10^{-22} and 6.0×10^{-22} $m^2/(sr^2)(J)$), respectively.

DISCUSSION

The upper limits of the cross section obtained from this experiment are reproduced in table II, together with the corresponding theoretical values predicted by Bolsterli (ref. 7), Talman (ref. 8), and Shima (ref. 9). An observed cross section recently reported by Adler and Cohen (ref. 12) is also included for comparison and discussion.

The geometry (unpublished data obtained from J. Talman), and ultimate cross-section resolution chosen for this experiment was based on Talman's original calculation which was later found to be too large by a factor of 500 (ref. 13). In addition, the calculation of Shima showed that the cross section was much more geometry dependent than predicted by either Bolsterli or Talman. In the geometry chosen, Shima's cross section was approximately one-tenth of that predicted by the others. Consequently, the results reported herein cannot be considered a rigorous test of the theoretically predicted values but represent only upper limits for the γ-2γ cross section. Information gained from this experiment, however, indicates that smaller cross sections in the range of the theoretical values can be measured with suitable improvement of the present technique.

The primary source strength can be increased substantially over that used in the present investigation. An increase of source strength by a factor of 10 to 2.5 curies ($\sim9\times10^{10}$ gamma rays/sec) can be accommodated with only slightly more complicated electronics. A more suitable geometry (90°, 90°, 135°) would increase the value of the cross section in copper from 0.1 to 4 nanobarns per steradians squared per MeV (0.062×10^{-24} to 2.5×10^{-24} $m^2/(sr^2)(J)$) but would reduce the detection efficiency by about a factor of 3 since it would necessitate moving the detectors further away from the target. Anticoincidence shielding of the gamma-ray detectors to eliminate cosmic-ray shower events would nearly eliminate the background events in the energy region of interest. Based on the present experimental results and by extrapolating to the new geometry, the

minimum number of sum-coincidence events that could be seen at the 95 percent confidence level in the absence of cosmic-ray background would be approximately one-fifth of the present number. Counting for a period of time about four times longer would gain at least a factor of 2 in sensitivity. The net gain in sensitivity therefore would be at least $[10\times(1/3)\times5\times2] = 33$. Therefore, a cross section in copper equal to or greater than about 4 nanobarns per steradian square per MeV could be detected. This is very nearly the theoretically predicted differential cross section for the γ-2γ process in copper target material in the new geometry.

The experiment of Adler and Cohen (ref. 12) has incorporated some of these improvements, but their choice of primary gamma-ray energy was unfavorable for an absolute determination of the cross section. As mentioned previously, if $E_0 > 1.02$ MeV (1.64×10^{-13} J), chance-true coincidence events can occur and have an energy sum of 1.15 MeV (1.84×10^{-12} J) independent of E_0. The source employed by Adler and Cohen (ref. 12) had $E_0 = 1.11$ MeV (1.78×10^{-13} J); therefore, it is possible that chance-true events were mistaken to be γ-2γ events. This is especially germane since they observed a cross section over 50 times larger than that theoretically predicted by Shima for the corresponding geometry. (Adler and Cohen reported a cross-section value six times larger than that predicted by an equation attributed to Shima of NASA Goddard Space Flight Center, Greenbelt, Maryland. However, private communication with Shima revealed that there was an error in their computation.) One method of determining whether the observed events were true γ-2γ events would be to vary the source strength. Adler and Cohen made no mention of having tested the results against source strength.

Because of the restriction that E_0 must be greater than 0.80 MeV (1.28×10^{-13} J) and other considerations such as decay scheme, half life, and availability, the manganese 54 and cobalt 60 isotopes seem to be the most suitable. Of these two, cobalt 60 is a better choice based on the energy dependence of the cross section.

CONCLUSIONS

A detection system combining energy-summing and time-coincidence techniques was applied in a search for the nuclear γ-2γ process. The double requirement allows the detection of this process in presence of other processes which have approximately 10^8 times larger cross sections.

The geometry chosen was one in which the two secondary gamma rays were emitted at an angle of 90° to each other and at an angle of 135° to the projection of the incident gamma-ray arrival direction. The primary gamma ray (1.33 MeV, 2.14×10^{-13} J) was obtained from radioactive cobalt 60. Statistically significant upper limits of 960 nanobarns per steradian squared per MeV (6×10^{-22} $m^2/(sr^2)(J)$) for the cross section with lead nuclei and 146 nanobarns per steradian squared per MeV (0.915×10^{-22} $m^2/(sr^2)(J)$)

for that with the copper nuclei were obtained, comparing with the theoretical values of 0.8 and 0.1 nanobarn per steradian squared per MeV (0.05×10^{-24} and 0.00625×10^{-24} $m^2/(sr^2)(J)$), respectively.

The upper limits established herein did not become a rigorous test of the theory. Information gained from this experiment, however, indicates that the theoretically predicted value of cross section can be measured, with suitable improvements of the present detection system, in a more favorable geometry.

Lewis Research Center,
National Aeronautics and Space Administration,
Cleveland, Ohio, March 8, 1967,
129-01-02-04-22.

APPENDIX A

SYMBOLS

A	frontal area of absorber
E	gamma-ray energy, MeV (J)
E_A	annihilation gamma-ray energy, MeV (J)
E_c	Compton scattered primary gamma-ray energy, MeV (J)
E_i	center energy of channel, MeV (J)
E_0	primary gamma-ray energy, MeV (J)
E_1, E_2	secondary gamma-ray energies, MeV (J)
ΔE	energy discrimination window
i, j, k	pulse-height intervals
m_0c^2	rest energy of electron, 0.511 MeV (0.82×10^{-13} J)
$N(E_0)$	observed number of sum coincidence events
N_γ	total number of primary gamma rays that interact in target during period of observation
$p(\Delta E, E_0)$	average detection efficiency, sr^2
$q(E_1, E_0)$	average probability that pair of gamma rays of energies E_1 and E_2 can escape from absorber without suffering energy degradation
R_{ch}	chance-coincidence rate
R_k	chance-sum pulse-height occurrence rate
R_1, R_2	average arrival rates of two random pulse trains or average rate at which gamma rays interact in target
R_{1i}	average arrival rates of pulses in pulse train 1
R_{2j}	average arrival rate of pulses in pulse train 2
r	mean source to target distance
S_0	primary source strength
T	counting period, sec
x, y, z	coordinates
x_0, y_0, z_0	target dimensions

$dx\ dy\ dz$	volume
$dy\ dz\ x_0$	volume located at y, z
γ	photon
δE	energy corresponding to one channel
$\epsilon(E_1), \epsilon(E_2)$	photo-peak detection efficiency for detecting gamma rays of energy E_1 or E_2 in any given geometry
θ_1, θ_2	mean angles with respect to center of target and projection of primary photon arrival direction, deg
θ_{12}	mean angle between detectors with vertex at target, deg
μ	total linear absorption coefficient in absorber for primary gamma-ray energy
ρ	mean target to detector distance
$d\sigma_{2\gamma}/d\Omega_1\, d\Omega_2$	γ-2γ cross section, nb/sr^2 (m^2/sr^2)
$d^3\sigma_{2\gamma}/d\Omega_1\, d\Omega_2\, dE_1$	differential γ-2γ cross section, nb/sr^2-MeV (m^2/sr^2-J)
$\overline{d^3\sigma_{2\gamma}/d\Omega_1\, d\Omega_2\, dE}$	average differential γ-2γ cross section, nb/sr^2-MeV (m^2/sr^2-J)
σ_T	total gamma-ray interaction cross section, nb/atom (m^2/atom)
$\varphi(E)$	photon flux
Subscripts:	
0	primary
1	first detector
2	second detector

APPENDIX B

CALCULATION OF OBSERVABLE NUMBER OF COINCIDENCE EVENTS

The observed number of sum coincidence events $N(E_0)$, associated with the γ-2γ process, which deposit the total primary gamma-ray energy E_0 in two detectors can be computed from the equation

$$N(E_0) = \left[\frac{A}{4\pi r^2}\left(1 - e^{-\mu y_0}\right)\int_0^T S_0(t)dt\right] \times \frac{1}{\sigma_T}\int_{(E_0-\Delta E)/2}^{(E_0+\Delta E)/2} 2\,\frac{d^3\sigma_{2\gamma}}{d\Omega_1\, d\Omega_2\, dE_1}\,\epsilon_1(E_1)\epsilon_2(E_2)\bar{q}(E_1, E_0)dE_1 \qquad \text{(B1)}$$

where $A/4\pi r^2$ is the solid angle subtended by the absorber to the source, A is the frontal area of the absorber, r is the average source to absorber distance, $1 - e^{-\mu y_0}$ is the probability that a primary gamma ray interacts in the absorber by any mechanism, μ is the total gamma-ray linear absorption coefficient in the absorber for the primary gamma-ray energy, y is the physical length of the absorber, and $\int_0^T S_0(t)dt$ is the integrated number of source gamma rays emitted in the period of observation.

$$\int_0^T S_0(t)dt \approx S_0 T$$

if T is small compared with the half-life of the source.

A quantity N_γ can now be defined which equals the total number of primary gamma-ray interactions of all types in the target over a counting period T:

$$N_\gamma = \frac{A}{4\pi r^2}\left(1 - e^{-\mu y_0}\right)\int_0^T S_0(t)dt \qquad \text{(B2)}$$

The remainder of equation (B1) is the probability that any one interaction is a γ-2γ interaction which proceeds in the geometry chosen and is detected. The term σ_T is the total gamma-ray interaction cross section for a target nuclei in nanobarns per atom and $d^3\sigma_{2\gamma}/d\Omega_1\, d\Omega_2\, dE_1$ is the differential γ-2γ cross section for the average geometry, assumed, for simplicity, to be constant over the solid angles subtended by each detector

to the target. A more exact evaluation would be necessary if a more quantitative result were required by the experiment. The terms $\epsilon_1(E_1)$ and $\epsilon_2(E_2)$ are photopeak detection efficiencies in steradians for detectors located at a distance of 10.15 centimeters from a point source of gamma rays of energies E_1 and E_2, respectively. In the calculation, it is assumed that the distance is equal to the mean absorber to detector distance. The term $\bar{q}(E_1, E_0)$ is the average probability that a pair of gamma rays of energies E_1 and E_2 (equal to $E_0 - E_1$) can escape from the absorber without suffering energy degradation. The factor 2 is necessary to account for the fact that either gamma ray can go into either detector while the other gamma ray is confined to entering the remaining detector if a coincidence is to occur. The integral is performed over an energy interval ΔE defined by the discrimination window.

A calculation of $\bar{q}(E_1, E_0)$, in a target in which pairs of gamma rays of energy E_1 and E_2 (equal to $E_0 - E_1$) are uniformly produced throughout the volume of the target, was performed. Figure 7 shows such a target. The probability that a pair of gamma rays can escape from the target at angles θ_1 and θ_2 from a volume dx dy dz situated at x, y, z is

$$r(x, E_1) = e^{-\mu_1 s/\sin\theta_1} e^{-\mu_2 (x_0 - x)/\sin\theta_2} \tag{B3}$$

where μ_1 and μ_2 are the linear gamma-ray absorption coefficient in the target for gamma rays of energy E_1 and E_2, respectively. The average probability $\bar{q}(E_1, E_0)$ that a pair of gamma rays emitted from the volume dy dz x_0 located at y, z can escape from the target is

$$\bar{q}(E_1, E_0) = \frac{1}{x_0} \int_0^{x_0} r(x, E_1) dx$$

$$= \frac{\dfrac{e^{-\mu_2 x_0}}{\sin\theta_2} - \dfrac{e^{-\mu_1 x_0}}{\sin\theta_1}}{x_0 \left(\dfrac{\mu_1}{\sin\theta_1} - \dfrac{\mu_2}{\sin\theta_2} \right)} \tag{B4}$$

except when

$$\frac{\mu_1}{\sin\theta_1} = \frac{\mu_2}{\sin\theta_2}$$

in which case,

$$\bar{q}(E_1, E_0) = e^{-\mu_1 x_0 / \sin\theta_1} \tag{B5}$$

For a target whose y_0 and z_0 dimensions are large compared with x_0 and small compared with the detector-target distance, equations (B4) and (B5) represent the average escape probability to a high degree of accuracy.

Table III tabulates the calculated values of $\bar{q}(E_1, E_0)$ for various energies for lead and copper targets ~0.319 centimeter thick ($x_0 = 0.319$ cm), $\theta_1 = \theta_2 = 135^\circ$, and $E_0 = 1.33$ MeV (2.14×10^{-13} J). The solid angle detection efficiency

$$p(E_1, E_0) = 2\epsilon_1(E_1)\epsilon_2(E_2)\bar{q}(E_1, E_0)$$

is also tabulated. Figure 8 is a plot of detection efficiency as a function of E_1/E_0 for $E_0 = 1.33$ MeV (2.14×10^{-13} J) in lead and copper. Here, $p(E_1, E_0)$ is symmetric about $E_0/2$. As shown in this figure, $p(E_1, E_0)$ is a slowly varying function of E_1 in the region of $E_1 = E_0/2$. Figure 2(b) shows that $d^3\sigma_{2\gamma}/d\Omega_1\, d\Omega_2\, dE_1$ is also a slowly varying function of E_1 near $E_0/2$. Consequently, the integral may be approximated by the quantity

$$\frac{\overline{d^3\sigma_{2\gamma}}}{d\Omega_1\, d\Omega_2\, dE} \cdot \Delta E \cdot p(\Delta E, E_0)$$

where $\overline{d^3\sigma_{2\gamma}}/d\Omega_1\, d\Omega_2\, dE$ and $p(\Delta E, E_0)$ are the average values of the γ-2γ differential cross section and the detection efficiency over the energy interval ΔE.

The quantity

$$\frac{1}{\sigma_T} \cdot \frac{\overline{d^3\sigma_{2\gamma}}}{d\Omega_1\, d\Omega_2\, dE} \cdot \Delta E$$

is the probability per steradian squared that any one interaction in the target is a γ-2γ interaction in which the secondary gamma rays have energies in the interval ΔE and are emitted into the solid angles $d\Omega_1\, d\Omega_2$ subtended by the detectors to the target. The term $p(\Delta E, E_0)$ is the average value of the product of photopeak detection probability for pairs of gamma rays of energy $E_1 + E_2 = E_0$, detector solid angles, and escape probability over ΔE. The average differential cross section over ΔE can therefore be computed from the equation

$$\frac{\overline{d^3\sigma_{2\gamma}}}{d\Omega_1\, d\Omega_2\, dE} = \frac{\sigma_T N(E_0)}{N_\gamma \cdot \Delta E \cdot p(\Delta E, E_0)} \tag{B6}$$

APPENDIX C

METHOD OF GENERATING CHANCE-COINCIDENCE SPECTRA

If two pulse trains in which the pulses are τ seconds long and randomly distributed in time are presented to a coincidence circuit, the resultant chance coincidence rate is

$$R_{ch} = 2\tau R_1 R_2$$

where R_1 and R_2 are the average arrival rates of the two random pulse trains. If, in addition to having a random distribution in time, there is also a distribution in pulse size and if the pulses are linearly added so that a coincident pair produces a pulse whose height is proportional to the sum of the pulse heights of the two pulses which generated it, a chance-sum pulse-height distribution is generated.

Let two pulse-height distributions R_{1i} and R_{2j} exist where R_{1i} is the average arrival rate of pulses in pulse train 1 having pulse heights between $E_i - (\delta E/2)$ and $E_i + (\delta E/2)$ and where R_{2j} is similarly defined. To determine the chance-coincidence occurrence rate for sum pulses lying in a pulse-height interval $E_k \pm (\delta E/2)$, all chance-coincidence events that contribute sum pulses in the interval k must be added to determine the chance-coincidence rate for the generation of sum pulses in the pulse-height interval k. For example, the chance-coincidence occurrence rate for pulses in the pulse-height interval $i = j = 1$ is $2\tau R_{11} R_{21}$ and these sum pulses have a pulse-height distribution extending from zero to $2\delta E$. If R_{1i} and R_{2j} vary slowly with i and j, about half of these events will lie in pulse-height interval $k = 1$ with the remainder lying in pulse-height interval $k = 2$. The chance-coincidence rate occurring between pulses in pulse-height intervals $i = 1$ and $j = 2$ and $i = 2$ and $j = 1$ will result in a chance-coincidence rate $2\tau(R_{11}R_{22} + R_{12}R_{21})$ for sum pulses lying in pulse-height interval between δE and $3\delta E$. Of these, about half will lie in pulse-height interval $k = 2$ with the remainder in $k = 3$. Thus, a general expression for the chance-coincidence occurrence rate of sum pulses in the k^{th} interval may be formulated as follows:

$$R_1 = \tau R_{11} R_{21}$$

$$R_2 = \tau\left[R_{11} R_{21} + (R_{11} R_{22} + R_{12} R_{21})\right]$$

$$R_3 = \tau\left[(R_{11} R_{22} + R_{12} R_{21}) + (R_{11} R_{23} + R_{12} R_{22} + R_{13} R_{21})\right]$$

$$\vdots \qquad\qquad \vdots$$

$$R_k = \tau\left[\sum_{i=1}^{k-1} R_{1i} R_{2(k-i)} + \sum_{i=1}^{k} R_{1i} R_{2(k+1-i)}\right]$$

In this experiment, the pulse-height distributions from two detectors were linearly added and then gated into a multichannel pulse-height analyzer if the individual pulses satisfied both pulse-height discriminator and time-coincidence requirements. Because certain events satisfying the time-coincidence requirement were of a chance origin, a chance-sum-coincidence pulse-height distribution was gated into the analyzer in addition to the true-coincidence pulse-height distribution. To separate the chance-coincidence pulse-height distribution from that of the true, a computer code was written to generate the chance-sum pulse-height occurrence rate R_k. In this code, R_{1i} and R_{2j} were defined on the interval $0 \leq i$ and $j \leq 2n$, where R_{1i} and R_{2j} are equivalent to zero for $n < i$, $j \leq 2n$, and $i = 0$. The values of R_{1i} and R_{2j} were obtained by measuring the gated pulse-height distribution from each of the detectors. In computing R_k, the indices i, j, and k referred to the analyzer channel number.

REFERENCES

1. Triebwasser, Sol; Dayhoff, Edward S.; and Lamb, Willis E., Jr.: Fine Structure of the Hydrogen Atom. V. Phys. Rev., vol. 89, no. 1, Jan. 1, 1953, pp. 98-106.
2. Layzer, Arthur J.: New Theoretical Value for the Lamb Shift. Phys. Rev. Letters, vol. 4, no. 11, June 1, 1960, pp. 580-582.
3. Euler, H.: Scattering of Light by Light. Ann. d. Physik, vol. 26, no. 5, July 1936, pp. 398-448.
4. Karplus, Robert; and Neuman, Maurice: The Scattering of Light by Light. Phys. Rev., vol. 83, no. 4, Aug. 15, 1951, pp. 776-784.
5. Delbrück, M.: Zusatz bei der Korrektur. Z. Physik, vol. 84, July 26, 1933, p. 144.
6. Sannikov, S. S.: Inelastic Scattering of Photons in the Coulomb Field of a Nucleus. Soviet Phys. JETP, vol. 15, no. 1, July 1962, pp. 196-198.
7. Bolsterli, Mark: Photon Splitting in a Nuclear Electrostatic Field. Phys. Rev., vol. 94, no. 2, Apr. 15, 1954, pp. 367-368.
8. Talman, James D.: Possibility of Observing a Nonlinear Electromagnetic Effect. Phys. Rev., vol. 139, no. 6B, Sept. 20, 1965, pp. 1644-1645.
9. Shima, Yaakov: Photon Splitting in a Nuclear Electric Field. Phys. Rev., vol. 142, no. 4, Feb. 25, 1966, pp. 944-956.
10. Moffatt, J.; and Stringfellow, M. W.: The Small Angle Scattering of High Energy Photons in Uranium. Phil. Mag., vol. 3, no. 29, May 1958, pp. 540-542.
11. Bösch, R.; Lang, J.; Müller, R.; and Wölfli, W.: Phys. Letters, vol. 2, no. 1, Aug. 1, 1962, pp. 16-17.
12. Adler, A. W.; and Cohen, S. G.: Search for the Splitting of Gamma-Ray Photons in the Electric Field of the Nucleus. Phys. Rev., vol. 146, no. 4, June 24, 1966, pp. 1001-1003.
13. Talman, James D.: Possibility of Observing a Nonlinear Electromagnetic Effect. Phys. Rev., vol. 141, no. 4, Jan. 1966, p. 1582.
14. Storm, Ellery; Gilbert, Eugene; and Israel, Harvey: Gamma-Ray Absorption Coefficients for Elements 1 through 100 Derived from the Theoretical Values of the National Bureau of Standards. Rep. No. La-2237, Los Alamos Scientific Lab., Univ. California, Apr. 1957.

15. Vegors, Stanley H., Jr.; Marsden, Louis L.; and Heath, R. L.: Calculated Efficiencies of Cylindrical Radiation Detectors. Rep. No. IDO-16370, Phillips Petroleum Co., Sept. 1, 1958.

16. Miller, W. F.; Reynolds, John; and Snow, William J.: Efficiencies and Photofractions for Sodium-Iodide Crystals. Rev. Sci. Instr., vol. 28, no. 9, Sept. 1957, pp. 717-719.

TABLE I. - COMPUTED AVERAGE DIFFERENTIAL CROSS SECTIONS

[Primary gamma-ray energy, E_0, 1.33 MeV (2.14×10^{-13} J).]

Target nuclei	Nuclear charge	Observable number of sum coincidence events, $N(\epsilon_0)$	Total number of gamma rays that interact in target, N_γ	Total gamma ray interaction cross section, σ_T	Energy discrimination window, ΔE	Average detection efficiency, $p(\Delta E, E_0)$	Computed average differential cross section, $\frac{\overline{d^3\sigma_{2\gamma}}}{d\Omega_1\, d\Omega_2\, dE}$
				U.S. Customary Units			
				nb	MeV	sr^2	$nb/(sr^2)(MeV)$
Copper	29	30	7.5×10^{11}	5.35×10^{9}	0.440	3.4×10^{-3}	146
Lead	82	50	9.0×10^{11}	18.5×10^{9}	.440	2.5×10^{-3}	960
				International System of Units			
				m^2	J	sr^2	$m^2/(sr^2)(J)$
Copper	25	30	7.5×10^{11}	5.35×10^{-28}	0.71×10^{-13}	3.4×10^{-3}	146
Lead	82	50	9.0×10^{11}	18.5×10^{-28}	$.7\times10^{-13}$	2.5×10^{-3}	960

TABLE II. - COMPARISON OF THEORETICAL DIFFERENTIAL CROSS SECTIONS AND EXPERIMENTALLY DETERMINED UPPER LIMITS

Target nuclei	Primary gamma ray energy, E_0	Geometry	This report	Adler and Cohen (ref. 12)	Bolsterli (ref. 7)	Talman (ref. 8)	Shima (ref. 9)
			Differential cross section, $\overline{d^3\sigma_{2\gamma}}/d\Omega_1\, d\Omega_2\, dE$				
	U.S. Customary Units						
	MeV	deg	nb/(sr^2)(MeV)				
Copper	1.33	135, 135, 90	146	--	1.0	0.8	0.1
Lead	1.33	135, 135, 90	960	--	8.0	6.0	.8
Copper-cobalt	1.11	105, 105, 130	---	50	.8	---	1.0
	International System of Units						
	J	deg	$m^2/(sr^2)(J)$				
Copper	2.14×10^{-13}	135, 135, 90	0.915×10^{-22}	---------	0.625×10^{-24}	0.5×10^{-24}	0.0625×10^{-24}
Lead	2.14	135, 135, 90	6.0×10^{-22}	---------	5.0	3.75×10^{-24}	.5
Copper-cobalt	1.78	105, 105, 130	----------	3.1×10^{-24}	.5	----------	.625

TABLE III. - DETECTION EFFICIENCIES FOR LEAD AND COPPER

TARGET MATERIAL IN GEOMETRY EMPLOYED

[Target thickness, 0.319 cm; primary gamma-ray energy, 1.33 MeV (2.14×10^{-13} J); $E_1 + E_2 = E_0$.]

(a) Lead

Ratio of detected gamma-ray energies to primary gamma-ray energies		Gamma ray linear absorption coefficient, cm^{-1} (a)		Average escape probability, $\bar{q}(E_1, E_0)$	Sodium iodide detection efficiencies, sr (b)		Calculated detection efficiencies as function of gamma-ray energy, $p(E_1, E_0)$
Detector 1, E_1/E_0	Detector 2, E_2/E_0	$\mu(E_1)$	$\mu(E_2)$		$\epsilon(E_1)$	$\epsilon(E_2)$	
0.1	0.9	30	0.71	0.05	0.167	0.0252	0.42×10^{-3}
.2	.8	5.8	.78	.28	.125	.0283	1.98
.3	.7	2.5	.87	.478	.079	.0326	2.46
.4	.6	1.62	1.02	.561	.061	.037	2.53
.5	.5	1.21	1.21	.581	.0465	.0465	2.51

(b) Copper

0.1	0.9	2.46	0.475	0.535	0.167	0.0252	4.50×10^{-3}
.2	.8	1.10	.505	.697	.125	.0283	4.94
.3	.7	.845	.545	.732	.079	.0326	3.77
.4	.6	.72	.58	.755	.061	.037	3.41
.5	.5	.63	.63	.754	.0465	.0465	3.26

[a] Values of $\mu_1(E)$ and $\mu_2(E)$ taken from ref. 14.

[b] Values of $\epsilon_1(E)$ and $\epsilon_2(E)$ taken from refs. 15 and 16.

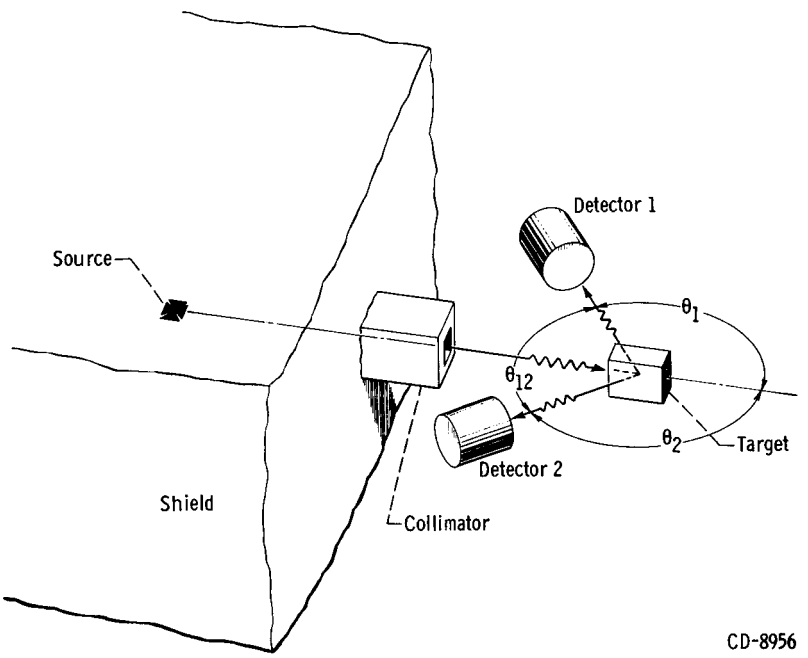

Figure 1. - General geometry employed.

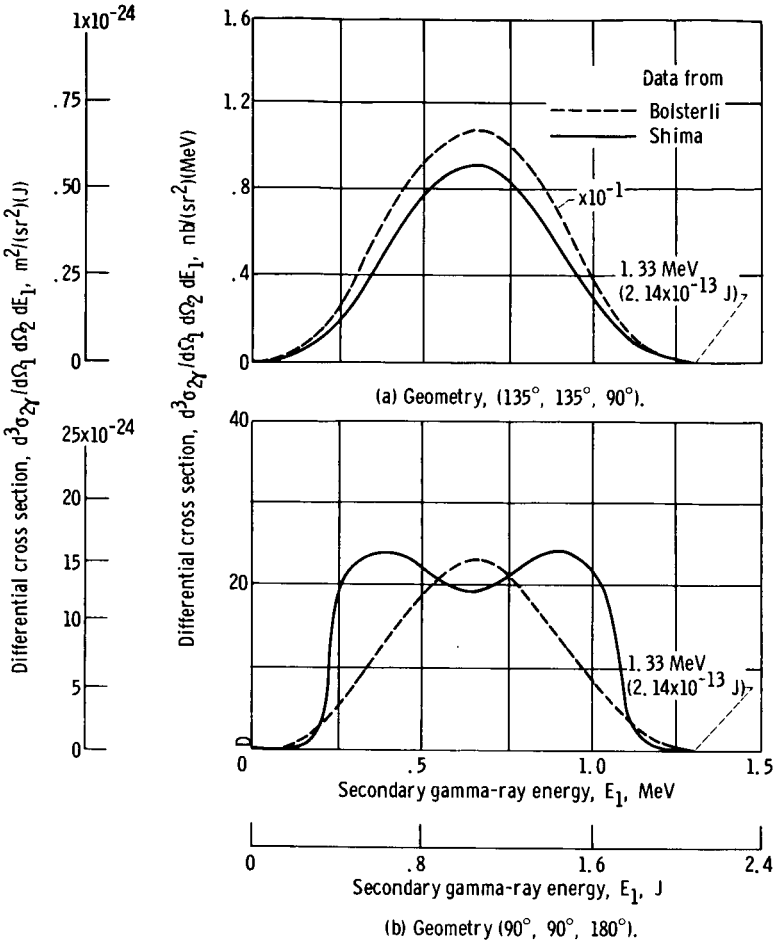

Figure 2. - Comparison of differential (γ - 2γ) cross sections as calculated for lead absorber and primary gamma-ray energy of 1.33 MeV (2.14×10^{-13} J).

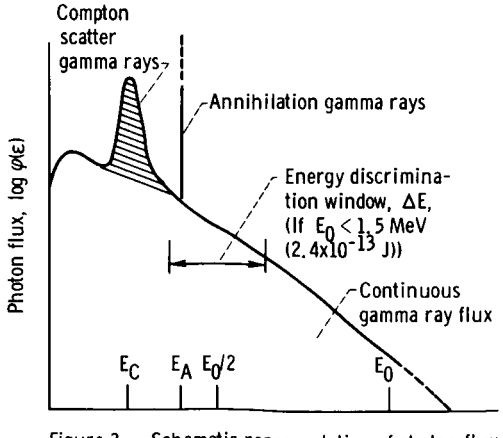

Figure 3. - Schematic representation of photon flux incident on gamma-ray detector. Average Compton scattered gamma ray energy, E_C; annihilation gamma ray energy, E_A; primary gamma ray energy, E_0.

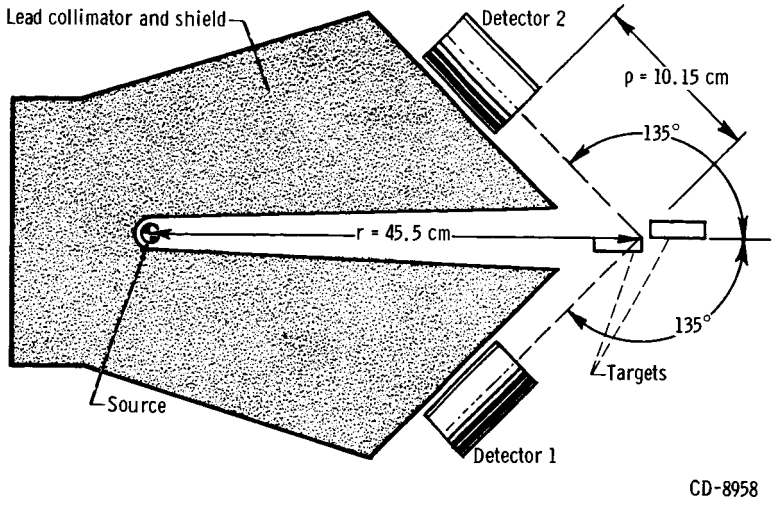

Figure 4. - Actual geometry employed in all measurements.

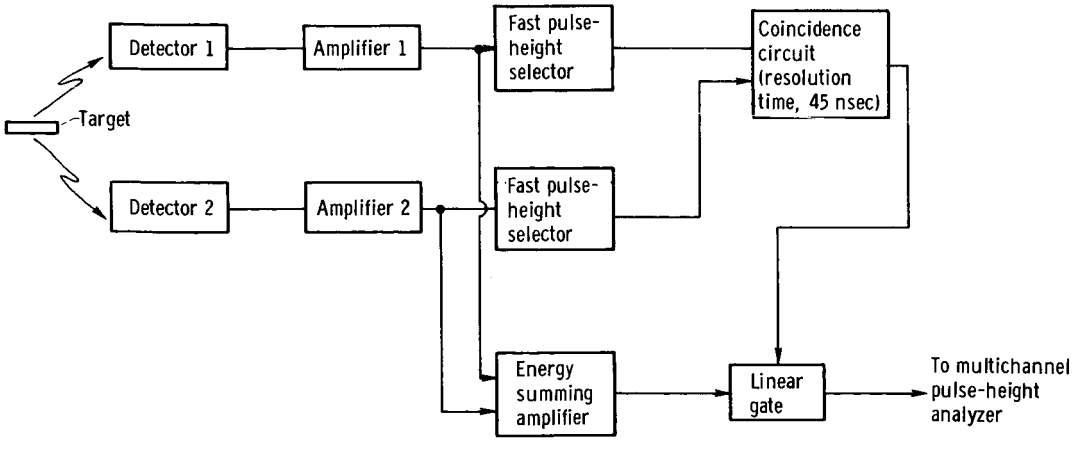

Figure 5. - Block diagram of electronics.

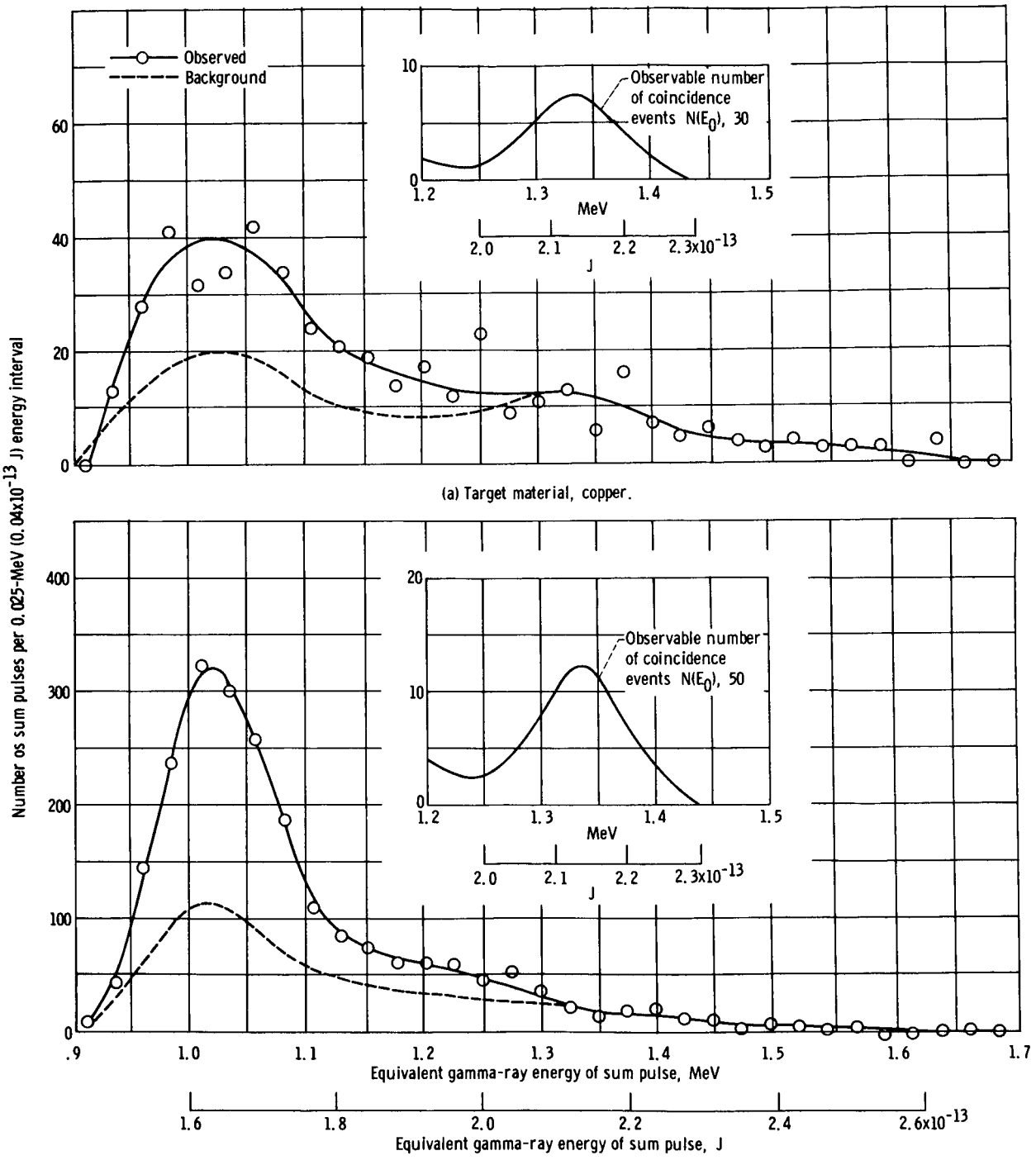

Figure 6. - Experimental sum-pulse distributions. Insets show shape of sum pulse observable at 95-percent significance level in presence of background shown.

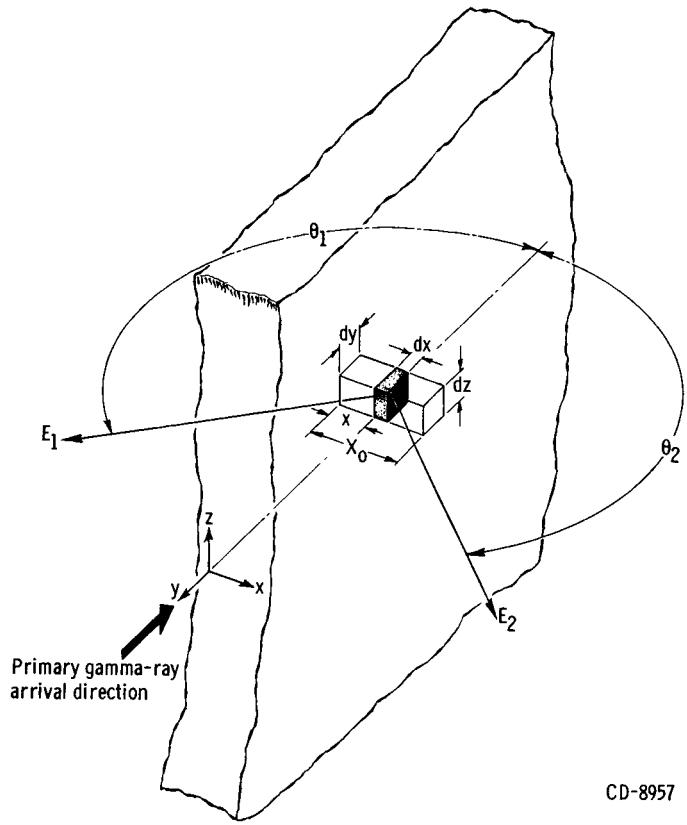

Figure 7. - Segment of target material.

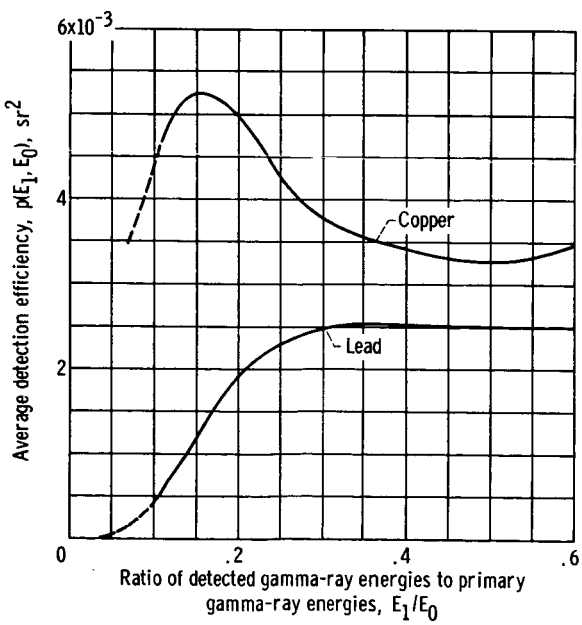

Figure 8. - Detection efficiencies for copper and lead targets 0.319-centimeter thick. Primary gamma-ray energy, 1.33 MeV (2.14×10^{-13} J).